



## A COHESIVE ZONE MODEL FOR CRACKS TERMINATING AT A BIMATERIAL INTERFACE

ALBERTO ROMEO and ROBERTO BALLARINI

Department of Civil Engineering, Case Western Reserve University, 10,900 Euclid Avenue,  
Cleveland, Ohio 44106-7201, USA

(Received 24 October 1995; in revised form 24 June 1996)

**Abstract**—Linear elastic fracture mechanics (LEFM) does not provide a realistic propagation criterion for a crack tip touching a bimaterial interface. In fact, LEFM predicts that the crack penetrates the interface at either zero or infinite value of the characteristic applied load, depending on the relative stiffness of the bonded materials. This paper presents a cohesive zone model that provides a propagation criterion for such cracks in terms of the parameters that define the relation between the crack opening displacement and the traction acting along the crack surfaces. Extensive numerical results are presented for the case of constant cohesive traction,  $\sigma_o$ , associated with a critical crack tip opening displacement,  $\eta_c$ . A quantitative evaluation of the effective toughening resulting from the presence of the interface is presented, for both small scale and large scale bridging, in terms of the Dundurs parameters ( $\alpha$  and  $\beta$ ), and  $\rho_2/L$ , where  $\rho_2$  is proportional to the small scale critical cohesive zone length and  $L$  is a characteristic length of the crack problem. In particular, universal results for small scale bridging are presented as

$$k_c = \sigma_o \left( \frac{\rho_2}{B^*(\alpha, \beta)} \right)^\lambda, \quad \delta_c = \frac{A(\alpha, \beta)}{B^*(\alpha, \beta)} \rho_2$$

where  $k_c$  and  $\delta_c$  are, respectively the critical stress intensity factor and critical cohesive zone length,  $\lambda$  is the power of the stress singularity associated with the elastic crack touching the interface, and  $A$  and  $B^*$  are universal functions. These equations generalize those derived from the Dugdale model for a homogeneous medium. It is shown through the analysis of a finite length crack that for a relatively wide range of  $\alpha$ - $\beta$  and  $\rho_2/L$  values, the presence of the interface has a rather insignificant effect on the critical stress, and the elastic singularity associated with a crack terminating at the interface between two dissimilar elastic materials dominates the stress field within an extremely small near-tip region. © 1997 Elsevier Science Ltd. All rights reserved.

### NOMENCLATURE

LEFM	Linear elastic fracture mechanics
COD, $[u_x^{(0)}]$	Crack opening displacement
s.i.f.	Stress intensity factor
SSY	Small scale yielding
LSY	Large scale yielding
GDB	Generalized Dugdale-Barenblatt model for SSY
$\alpha, \beta$	Dundurs parameters
$\lambda$	Power of stress singularity at the interface
$\delta, \delta_c$	(Critical) extent of the plastic zone
$\mu_i$	Shear modulus
$\nu_i$	Poisson's ratio
$E_i^*$	Plane strain/plane stress elastic modulus
$G_i$	Strain energy release rate
$e$	Relative error
$r_{k,c}$	Extent of the k-dominated region
$\sigma^{(i)}$	Stress field
$\sigma_r, \sigma_{rc}, \sigma_c$	(Critical) remote stress
$\sigma_c^{hom}$	Critical remote stress for a homogeneous system
$k, k_c$	(Critical) far field stress intensity factor
$\sigma_o$	Yield stress
$K_{ij}$	Cauchy type kernels
$\eta, \eta_c, \eta_k, \eta_{\sigma_o}$	(Critical) COD at the interface
$\tilde{\eta}_k, \tilde{\eta}_{\sigma_o}$	Non dimensional COD at the interface
$K, K_k, K_{\sigma_o}$	Local s.i.f.
$f_k, f_{\sigma_o}, h, h^{hom}$	Non dimensional local s.i.f.

## 1. INTRODUCTION

Consider, as shown in Fig. 1, a crack terminating at the interface between two perfectly bonded linear elastic half-planes. The shear moduli, Poisson's ratios and critical energy release rates are, respectively,  $\mu_i$ ,  $\nu_i$  and  $G_i$  where subscript  $i$  ( $i = 1, 2$ ) denotes "material  $i$ ". As shown by Zak and Williams (1963), for loading symmetric with respect to the crack line, the stress at a point  $r = -\xi$  ahead of the crack tip can be written as

$$\sigma^{(2)} \propto kr^{-\lambda} \quad (1)$$

where the stress infinity factor,  $k$ , is a function of geometry, loading and elastic mismatch between the bonded materials, and  $\lambda$ , the power of the stress singularity, is the solution of the characteristic equation

$$\cos(\lambda\pi) = \frac{2(\beta - \alpha)}{(1 + \beta)}(1 - \lambda)^2 + \frac{\alpha + \beta^2}{1 - \beta^2} \quad 0 \leq \lambda < 1. \quad (2)$$

In eqn (2)  $\alpha$  and  $\beta$  are the Dundurs parameters (Dundurs, 1969), defined by

$$\alpha = \frac{\mu_2(\kappa_1 + 1) - \mu_1(\kappa_2 + 1)}{\mu_2(\kappa_1 + 1) + \mu_1(\kappa_2 + 1)}; \quad \beta = \frac{\mu_2(\kappa_1 - 1) - \mu_1(\kappa_2 - 1)}{\mu_2(\kappa_1 + 1) + \mu_1(\kappa_2 + 1)} \quad (3)$$

where

$$\kappa_i = 3 - 4\nu_i$$

for plane strain and

$$\kappa_i = \frac{3 - \nu_i}{1 + \nu_i}$$

for plane stress. The loci of constant  $\lambda$  in the  $\alpha$ - $\beta$  plane are plotted in Fig. 2a. As shown by Suga *et al.* (1988), the  $\beta$  values for an extensive number of relevant composite systems are arranged in a rather narrow band around the line  $\alpha = 4\beta$ , while the  $\alpha$  values span the entire domain. For this reason the calculations presented subsequently were performed for  $\alpha = 4\beta$ .

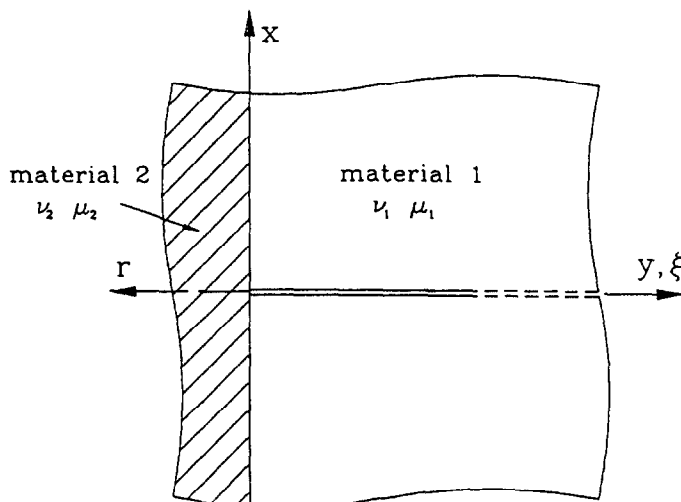


Fig. 1. Crack terminating at a bimaterial interface.

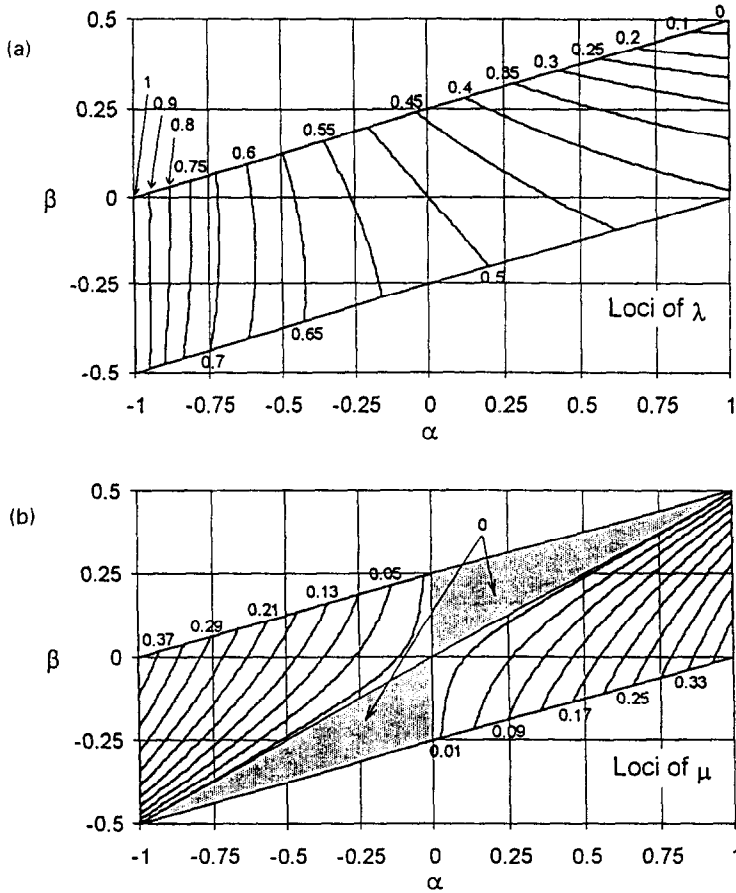


Fig. 2. (a) Loci of constant  $\lambda$  in the  $\alpha$ - $\beta$  plane. (b) Loci of constant  $\mu$  in the  $\alpha$ - $\beta$  plane.

The stress concentration at the tip of the crack shown in Fig. 1 can be relaxed by penetration through the interface, propagation along the interface, reflection, or a combination of these mechanisms. If the interface is not perfectly bonded, but is subjected to compressive residual stresses, the stress concentration can be relieved through frictional sliding along the interface. This latter mechanism was studied by Wang *et al.* (1991) using singular integral equations. This paper is concerned with predicting the loads necessary to extend the crack *through* the interface. This implies a “strong” interface.

Because  $k$  is not the same as the intensity factor  $K$  at the tip of a crack in a homogeneous material, the classical LEFM criterion  $K = K_c$  is not available to predict crack penetration through the interface. Even the standard energy release rate criterion is not appropriate. In fact, the energy release rate per unit thickness,  $G_2$ , associated with a virtual infinitesimal crack extension,  $\delta$ , through the interface is given by

$$G_2 \equiv \lim_{\delta \rightarrow 0} \frac{1/2 \int_{-\delta}^0 \sigma^{(2)} [u_x^{(2)}] d\xi}{\delta} \quad (4)$$

where  $\sigma^{(2)}$  is the stress ahead of the crack before the extension given by (1), and  $[u_x^{(2)}]$  represents the crack opening displacement (COD) of the extended crack, which, as shown in the Appendix, can be written as

$$[u_x^{(2)}(\xi)] = \frac{4k}{E_1} \delta^{1-\lambda} H(\xi/\delta; \alpha, \beta) \quad (5)$$

where  $H$  is a (non-dimensional) bounded function of position and the Dundurs parameters, and  $E_i = 8\mu_i/(1 + \kappa_i)$ . Substitution of (1) and (5) into (4) yields

$$G_2 \propto k^2 \lim_{\delta \rightarrow 0} \delta^{1-2\lambda}. \quad (6)$$

According to (6), as  $\delta \rightarrow 0$  the energy release rate becomes infinite for those bimaterial systems characterized by  $\lambda > 0.5$  ( $\mu_1 > \mu_2$ ), and zero for  $\lambda < 0.5$  ( $\mu_1 < \mu_2$ ). Therefore, LEFM predicts that the crack propagates through the interface under zero load for  $\mu_1 > \mu_2$  and infinite load for  $\mu_2 > \mu_1$ . An attempt at resolving this problem was made by Cook and Erdogan (1972), who proposed a fracture criterion based on the comparison of the elastic stresses in the composite medium with the corresponding critical stresses in the reference homogeneous systems. The method, which can be applied to a variety of propagation mechanisms such as through cleavage of medium 2, reflection in medium 1, or interfacial debonding, relies on the determination of a characteristic distance,  $r_w$ , at which stresses are compared. However, the determination of  $r_w$  which is associated with the materials' microstructure, is rather unclear.

Another important issue that has not been addressed systematically is the determination of the region of dominance of the stress intensity factor  $k$ . If this parameter is to be relevant in the assessment of the state of stress near a crack tip surrounded by damaged material, it should be associated with a "healthy" region of dominance. The results calculated in this paper show that the region dominated by  $k$  is extremely small if the crack is in the more compliant material. Thus for this case the linear elastic solution cannot be used to characterize crack initiation.

He and Hutchinson (1989), using singular integral equations, developed a model and criteria for predicting whether a crack that touches a bimaterial interface will penetrate the interface or be deflected along the interface. Their analysis eliminates the parameter  $k$  through the assumption that the putative extensions are of equal length, and therefore cannot be used to predict the loads needed to extend the crack in either direction.

In the present work, a cohesive zone model is developed in the spirit of Barrenblatt's original model (Barrenblatt 1962), which postulates the existence of an autonomous region (whose length is much smaller than any other characteristic length) along the crack surfaces which is subjected to tractions that resist crack opening. The relevant parameters in this model are those that define the relation between the crack opening displacements and the associated tractions. Moreover, the model can be (and has been) extended to cases where the length of the cohesive zone is not much smaller than the crack length and other characteristic dimensions. An example is the Dugdale model (Dugdale, 1962), which corresponds to a constant traction equal to the yield stress,  $\sigma_o$ , and the critical crack tip opening displacement,  $\eta_c$ . Barenblatt's model is intended to describe the cohesion which resists crack propagation, while Dugdale developed his model to predict the extent of crack tip plasticity in plane stress specimens of steel. However, the same mathematical techniques can be used to formulate and solve the boundary value problem associated with each model.

The model developed in this paper, which is formulated in terms of singular integral equations, extends Barenblatt's ideas to the case of a crack whose tip touches a bimaterial interface. The numerical calculations performed for a constant crack opening resisting traction therefore generalize the Dugdale yield strip model, for both large scale and small scale cohesive zone lengths. It is important to note that the model presented here does not suggest that crack propagation is accompanied by plastic deformation: the model is proposed for any material system and configuration that is characterized with inelastic deformation in the vicinity of the crack tip that is localized along a plane, and can therefore be approximated with a traction/crack opening displacement law. Material systems for which this type of modeling is generally acceptable include concrete and rock, whose cracks are

accompanied by microcracking, and polymers, which are associated with crazing. Regardless of the type of inelastic deformation, if the length of the cohesive zone is much smaller than any other characteristic lengths in the problem, the deformation will henceforth be referred to as small scale yielding (SSY). Otherwise it is termed large scale yielding (LSY). SSY (LSY) is associated with relatively small (large) values of the ratio

$$\frac{\rho_2}{L} \equiv \frac{\eta_c E_2'}{\sigma_o L} \quad (7)$$

where  $L$  is a characteristic length of the crack problem. In this study,  $\rho_2$ , which is proportional to the length of SSY plastic zone, is assumed to be a constant material property. The distinction between SSY and LSY is essential in this work because each requires a different computational scheme. A direct numerical integration of the integral equations governing the specific finite cohesive crack problem is appropriate for LSY conditions. For small crack tip deformation such an algorithm loses accuracy and an asymptotic crack analysis is recommended, which leads to a general SSY propagation criterion based on the introduction of the bimaterial toughness,  $k_c$ . The two methods are mutually complementary and the corresponding solutions show a smooth transition.

This paper is organized as follows. The next section provides a review of the assumptions and principal results of the Dugdale model. This is followed by a generalization of the model to bimaterial systems under SSY conditions. To assess the range of validity of the *universal* results obtained for SSY, the stresses ahead of a finite length crack calculated for general yielding conditions are compared with those predicted by the singular elastic solution. Finally, the critical stress associated with crack penetration, calculated as functions of elastic mismatch and the parameters that describe the inelastic deformation, is compared with the stress required to extend the crack in a homogeneous medium.

## 2. BRIEF REVIEW OF THE DUGDALE MODEL FOR HOMOGENEOUS SYSTEMS

The Dugdale model was first proposed for a Griffith crack of length  $2l$  embedded in an infinite homogeneous elastic-plastic plane under remote tension,  $\sigma$ . The zone of plastic deformation ahead of either crack tip is modeled as an extension,  $\delta$ , of the actual crack subjected to a constant closing pressure equal to the material yield stress,  $\sigma_o$ . This model relies on the superposition of two elastic solutions, a crack under remote tension and a crack with closure pressure near the tips. The equilibrium length of the plastic zone,  $\delta$ , is determined by requiring a zero stress singularity at the tip of the virtual crack extension. The following expressions result for  $\delta$  and for the crack opening displacement,  $\eta$ , at the tip of the actual crack.

$$\frac{\delta}{l} = \sec \frac{\pi\sigma}{2\sigma_o} - 1 \quad (8)$$

$$\frac{\eta}{l} = \frac{8\sigma_o}{\pi E'} \ln \left( \frac{\delta}{l} + 1 \right). \quad (9)$$

Equations (8) and (9) are exact for all  $\delta/l$  and thus apply to the general case of LSY. For SSY conditions,  $\delta/l \ll 1$ , they reduce to

$$\delta = \frac{\pi}{8} \left( \frac{K}{\sigma_o} \right)^2 \quad (10)$$

$$\eta = \frac{K^2}{E'\sigma_o} = \frac{G}{\sigma_o} \quad (11)$$

where  $K$  is the stress intensity factor due to the remote loading.

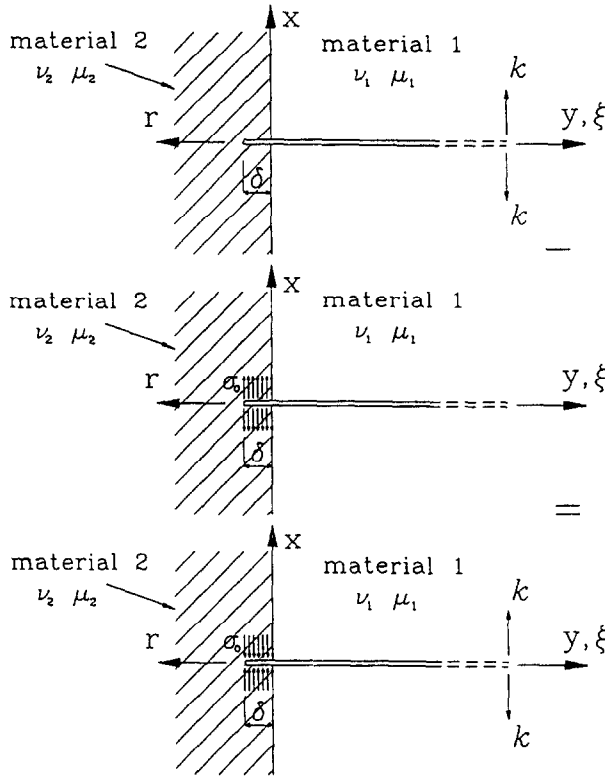


Fig. 3. Superposition scheme for a semi-infinite cohesive crack.

It is assumed that the crack propagates when the crack tip opening displacement,  $\eta$ , reaches a material constant critical value,  $\eta_c$ . Under SSY conditions the critical cohesive zone length,  $\delta_c$  and critical stress intensity factor,  $K_c$ , are

$$\delta_c = \frac{\pi E' \eta_c}{8 \sigma_o} \equiv \frac{\pi}{8} \rho \tag{12}$$

$$K_c = \sigma_o \left( \frac{E' \eta_c}{\sigma_o} \right)^{1/2} \equiv \sigma_o \rho^{1/2} \tag{13}$$

where  $\rho \equiv E' \eta_c / \sigma_o$  is a characteristic length of the material. Equation (11), as shown by Rice (1968), proves that the condition  $\eta_{ssy} = \eta_c$  is equivalent to the crack propagation criterion,  $K = K_c$ .

### 3. EXTENSION OF THE DUGDALE MODEL TO BIMATERIAL SYSTEMS UNDER SSY CONDITIONS

#### 3.1. SSY model

Consider a crack terminating at a bimaterial interface and assume that the inelastic deformation is confined to a line of length  $\delta$  beyond the bimaterial interface, such that  $\delta/L \ll 1$ , where  $L$  is a characteristic length of the problem. Assume that the bimaterial system remains in the elastic range elsewhere. This problem can be solved by means of an asymptotical analysis using the superposition scheme shown in Fig. 3. A semi-infinite crack whose tip is at a distance  $\delta$  beyond the interface is subjected to two loading conditions: a generic far-field loading given in terms of the applied remote stress intensity factor,  $k$ , (Fig. 3a), and a constant pressure,  $\sigma_o$  applied along the surfaces of the virtual crack extension through the interface (Fig. 3b).

It is important to note that for metals this scenario is applicable to plane stress situations; it is not applicable to plane strain situations, for which the yielding may occur

along inclined slip planes. However, the analytical model proposed here can be modified without major difficulties to handle either situation.

As shown by Atkinson (1975), He and Hutchinson (1989) and Romeo and Ballarini (1995), the stress infinity factor at the tip of the extended crack,  $K_k$ , and crack opening displacement at the interface,  $n_k$ , resulting from the remote loading are given by

$$K_k = k\delta^{1/2-\lambda}f_k(\alpha, \beta) \tag{14}$$

$$\eta_k = \frac{4k}{E_1'}\delta^{(1-\lambda)}\tilde{\eta}_k(\alpha, \beta) \tag{15}$$

where  $k$  corresponds to the stress infinity factor associated with the same crack terminating at the interface ( $\delta = 0$ ). For the second loading condition the corresponding quantities are given by

$$K_{\sigma_o} = \sigma_o\sqrt{2\pi\delta}f_{\sigma_o}(\alpha, \beta) \tag{16}$$

$$\eta_{\sigma_o} = \frac{4\sigma_o}{E_1'}\delta\tilde{\eta}_{\sigma_o}(\alpha, \beta). \tag{17}$$

A brief description of the singular integral equation techniques used by He and Hutchinson (1989) and Romeo and Ballarini (1995) to calculate functions  $f_k$ ,  $\tilde{\eta}_k$ , as well as necessary modifications used in this paper to calculate  $f_{\sigma_o}$  and  $\tilde{\eta}_{\sigma_o}$ , is included in the Appendix. The loci of constant values of these functions in the  $\alpha$ - $\beta$  plane are presented in Fig. 4a-d. For a homogeneous system ( $\alpha = \beta = 0$ )  $f_k = 1$ ,  $\tilde{\eta}_k = (2/\pi)^{1/2}$  and  $f_{\sigma_o} = \tilde{\eta}_{\sigma_o} = 2/\pi$ .

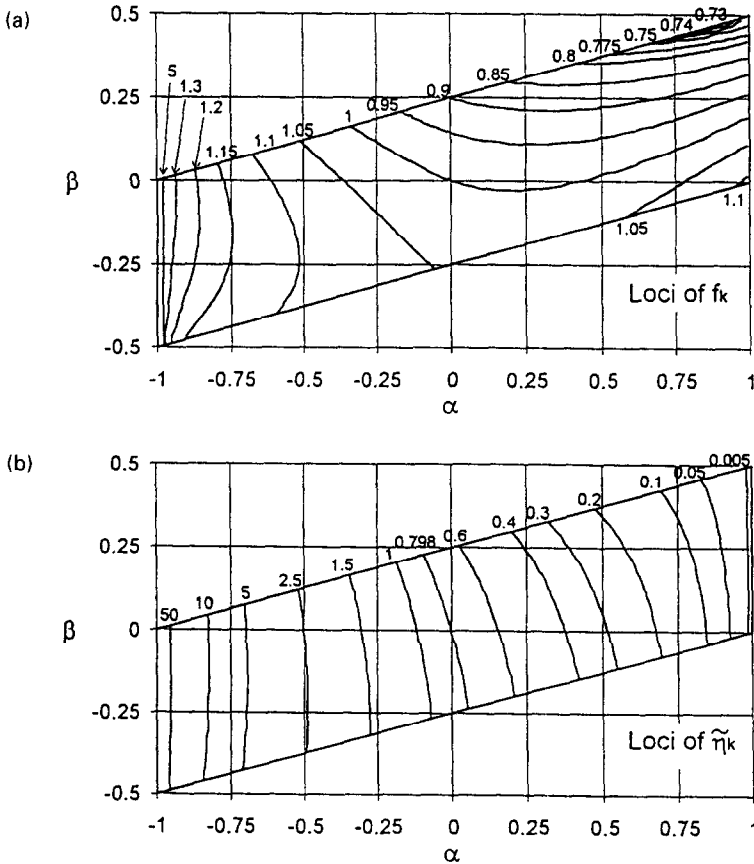


Fig. 4. (a) Loci of constant  $f_k$ , in the  $\alpha$ - $\beta$  plane. (b) Loci of constant  $\eta_k$ , in the  $\alpha$ - $\beta$  plane. (c) Loci of constant  $f_{\sigma_o}$ , in the  $\alpha$ - $\beta$  plane. (d) Loci of constant  $\tilde{\eta}_{\sigma_o}$ , in the  $\alpha$ - $\beta$  plane. (Continued overleaf.)

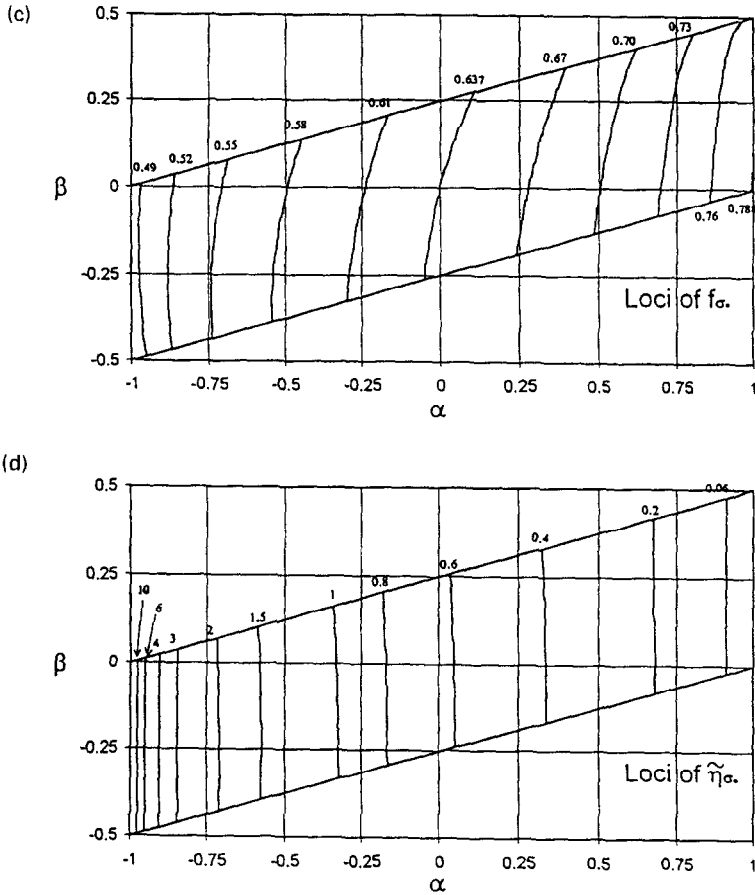


Fig. 4—continued.

The total stress intensity factor at the tip of the extended crack and the COD at the interface are given by

$$K_2 = K_k - K_{\sigma_o} \tag{18}$$

$$\eta = \eta_k - \eta_{\sigma_o} \tag{19}$$

For a given bimaterial system and a given value of  $K_2$ , (18)–(19) can be used to derive  $\delta$  and  $\eta$  as

$$\delta = (kf_k)^{1/2} [\sigma_o \sqrt{2\pi f_{\sigma_o}} + K_2 \delta^{-1/2}]^{-1/\lambda} \tag{20}$$

$$\eta = 4\delta \frac{\sigma_o}{E_1} \left[ \left( \sqrt{2\pi f_{\sigma_o}} + \frac{K_2}{\sigma_o \delta^{1/2}} \right)^{-1/\lambda} \frac{\tilde{\eta}_k}{f_k} - \tilde{\eta}_{\sigma_o} \right] \tag{21}$$

$K_2 = 0$  corresponds to a generalized Dugdale (GD) model, for which the resistance to the crack propagation relies entirely on the cohesive pressure,  $\sigma_o$ . For this case, (20) and (21) are explicit and reduce to

$$\delta = A(\alpha, \beta) \left( \frac{k}{\sigma_o} \right)^{1/2} \tag{22}$$

$$\eta = B(\alpha, \beta) \frac{\sigma_o}{E_1'} \left( \frac{k}{\sigma_o} \right)^{1/2} \tag{23}$$

where

$$A(\alpha, \beta) = \left( \frac{1}{\sqrt{2\pi} f_{\sigma_o}} \right)^{1/2} \tag{24}$$

$$B(\alpha, \beta) = 4A(\alpha, \beta) [\tilde{\eta}_k A(\alpha, \beta)^{-\lambda} - \tilde{\eta}_{\sigma_o}]. \tag{25}$$

The propagation criterion  $\eta = \eta_c$  (where  $\eta_c$  is a known medium 2 property independent of the bimaterial combination), applied to the crack opening displacement at the interface, can be used to obtain the value of the far-field stress intensity factor associated with crack propagation through the interface

$$k_c = \sigma_o^{1-\lambda} \left( \frac{\eta_c E_1'}{B} \right)^\lambda \equiv \left( \frac{C}{B} \right)^\lambda \sigma_o \rho_2^\lambda = \sigma_o \left( \frac{\rho_2}{B^*} \right)^\lambda \tag{26}$$

where

$$\rho_2 \equiv \frac{\eta_c E_2'}{\sigma_o}, \quad C \equiv \frac{1-\alpha}{1+\alpha}. \tag{27}$$

The non-dimensional critical length of the plastic zone,  $\delta_c$  is given by

$$\frac{\delta_c}{L} = \frac{A}{B} C \frac{\rho_2}{L} \equiv \frac{A}{B^*} \frac{\rho_2}{L}. \tag{28}$$

Equations (22), (23), (26), and (28) generalize to bimaterial systems the SSY results for homogeneous systems given, respectively, by (10), (11), (13) and (12). Note that the critical extent of the plastic zone is governed by  $\rho_2$  and the function of the Dundurs parameters  $AC/B$ . As for the homogeneous case, it is independent of the intensity of the remote load. A plot of (28) is shown in the boxed insert of Fig. 12, which illustrates that for a given  $\rho_2/L$  the critical cohesive zone length for positive values of  $\alpha$  is larger than for negative values.

### 3.2. Effective strengthening

The quantity  $k_c$  represents an effective fracture toughness associated with the presence of the interface. Since the physical dimensions of  $k_c$  show an  $\alpha$ - $\beta$  dependence through  $\lambda$ , a comparison of different bimaterial systems in terms of  $k_c$  is not appropriate. A comparison of bimaterial strengthening is, on the other hand, possible in terms of the critical nominal value of the far field stress,  $\sigma_c$  associated with  $k_c$ , which can be normalized with respect to  $\sigma_o$  as

$$\frac{\sigma_c}{\sigma_o} = \frac{1}{\sqrt{\pi} h(\alpha, \beta)} \frac{C^\lambda}{B^\lambda} \left( \frac{\rho_2}{L} \right)^\lambda \tag{29}$$

where  $h = k/(\sigma\sqrt{\pi}L^\lambda)$  represents the non-dimensional stress intensity factor and  $L$  is a characteristic length of the problem. Through (29) it is possible to express the ratio of  $\sigma_c$  for a crack at the interface of a given  $\alpha$ - $\beta$  system to the critical stress for the same crack in

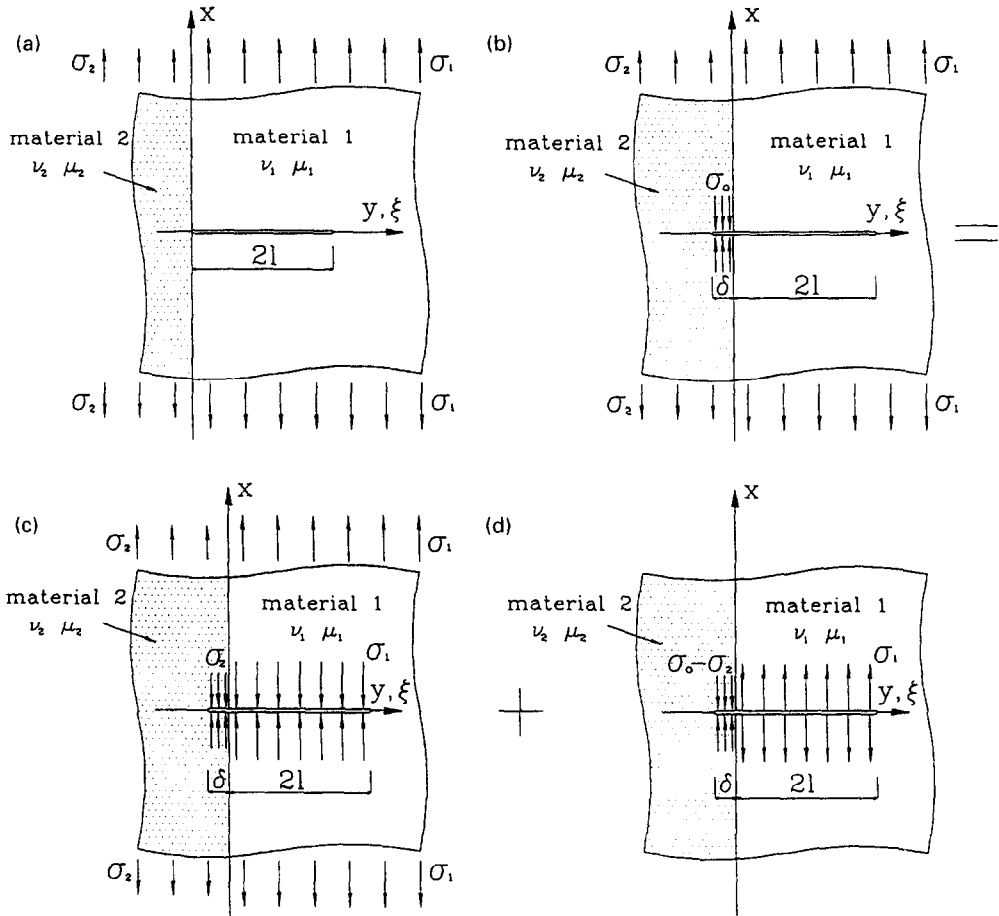


Fig. 5. Finite crack terminating at bimaterial interface (a) and superposition scheme for LSY (b-d).

a homogeneous medium 2,  $\sigma_c^{hom}$ , for which  $A(0,0) = \pi/8$ ,  $B(0,0) = 1$  and  $C(0,0) = 1$ . This ratio is given by

$$\frac{\sigma_c}{\sigma_c^{hom}} = \frac{h(0,0)C(\alpha, \beta)^\lambda \left(\frac{\rho_2}{L}\right)^{\lambda-1/2}}{h(\alpha, \beta)B(\alpha, \beta)^\lambda} \equiv \Theta(\alpha, \beta) \left(\frac{\rho_2}{L}\right)^{\lambda-1/2} \quad (30)$$

where  $\Theta$  for a given crack problem is a function of the Dundurs parameters only. Equation (30) provides a criterion to quantify the strengthening associated with the bimaterial interface. Those bimaterial systems that are characterized by

$$\Theta(\alpha, \beta) \left(\frac{\rho_2}{L}\right)^{\lambda-1/2} > 1 \quad (31)$$

exhibit a higher value of the critical load as compared to the reference homogeneous system. Note that for a homogeneous system the left hand side of (30) is identically 1.

3.3. Finite crack terminating at the interface and corresponding k dominance

As an application, consider a crack of length  $2l$  terminating at a bimaterial interface and subjected to constant remote tensile stresses,  $\sigma_1$  and  $\sigma_2$  such that

$$\sigma_1 = \frac{1-\alpha}{1+\alpha} \sigma_2 = C\sigma_2 \quad (32)$$

as shown in Fig. 5a. The stresses defined by (32) produce a uniform state of stress in the uncracked half-planes and correspond to a constant far-field displacement.

In order to determine the conditions under which the SSY model for the crack tip plastic effects is appropriate, it is first necessary to estimate the extent of the  $k$ -dominance for the elastic problem,  $\delta = 0$ . The region of  $k$ -dominance,  $r_{k,e}$ , is defined as the zone in front of the actual crack tip (Fig. 5a) in which the elastic stress field,  $\sigma^{(2)}(\xi)$ , is approximated by its leading singular term ( $k$ -solution) given by

$$\sigma_{asym}^{(2)} = \frac{k}{\sqrt{2\pi r'}} \tag{33}$$

to within a given relative error,  $e$

$$\left| \frac{\sigma^{(2)}(\xi) - \sigma_{asym}^{(2)}(\xi)}{\sigma(\xi)} \right| < e \quad 0 < -\xi \leq r_{k,e}. \tag{34}$$

The loci of the non-dimensional stress intensity factor

$$h(\alpha, \beta) = \frac{k}{\sigma_1 \sqrt{\pi l^\lambda}} \tag{35}$$

in the entire  $\alpha$ - $\beta$  plane, as calculated in Romeo and Ballarini (1994), are shown in Fig. 6. The values of  $h$  were found by means of a singular integral formulation of the elastic crack problem, which was also used to compute the full elastic stress field,  $\sigma^{(2)}(\xi)$ . As expected,  $r_{k,e}$  depends strongly on the elastic mismatch between the two bonded half-planes. Plots of the non-dimensional size of the  $k$ -dominated zone,  $r_{k,e}/l$ , vs  $\alpha$  for  $e = 5\%$ ,  $10\%$ ,  $15\%$  and  $20\%$  are presented in Fig. 7 for bimaterial systems characterized by  $\alpha = 4\beta$ . It is observed that a healthy  $k$ -dominance exists when the crack is in the stiffer material. The  $k$ -dominated region reaches in fact a peak for a bimaterial mismatch corresponding to  $\alpha \approx -0.7$  where it is as large as  $1/4$  of the crack length for  $e = 10\%$  and almost  $1.2$  of the crack length for  $e = 20\%$ . For homogeneous systems  $r_{k,e}$  is considerably lower than its peak value (about  $l/13$  for  $e = 10\%$  and  $l/6$  for  $e = 20\%$ ). When the crack is in the elastically softer material,  $r_{k,e}$  diminishes dramatically, and for  $\alpha > 0.5$  it almost vanishes.

Figure 7 can be used to determine upper bound values  $\rho_2/l_k$  for which the GD SSY model is applicable to the finite length crack problem shown in Fig. 5b. Since the SSY model requires that the zone of plastic deformation,  $\delta$ , be completely contained within the  $k$ -dominated region,  $\rho_2/l_k$  is determined by setting  $\delta \equiv r_{k,e}$  in (28). The results are presented in Fig. 8. For a given  $\rho_2$  and  $\alpha = 4\beta$ , this plot provides the shortest crack length for which the SSY analysis is expected to hold. For negative  $\alpha$  values the model applies not only to “brittle” cracks (small  $\rho_2/l$  values) but also to relatively “ductile” ones (large  $\rho_2/l$  values). For positive  $\alpha$  values the SSY model applies only to increasingly longer cracks, and virtually

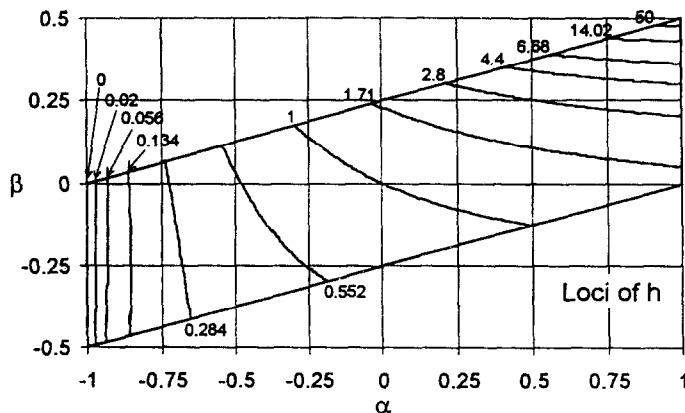


Fig. 6. Loci of constant  $h$  in the  $\alpha$ - $\beta$  plane.

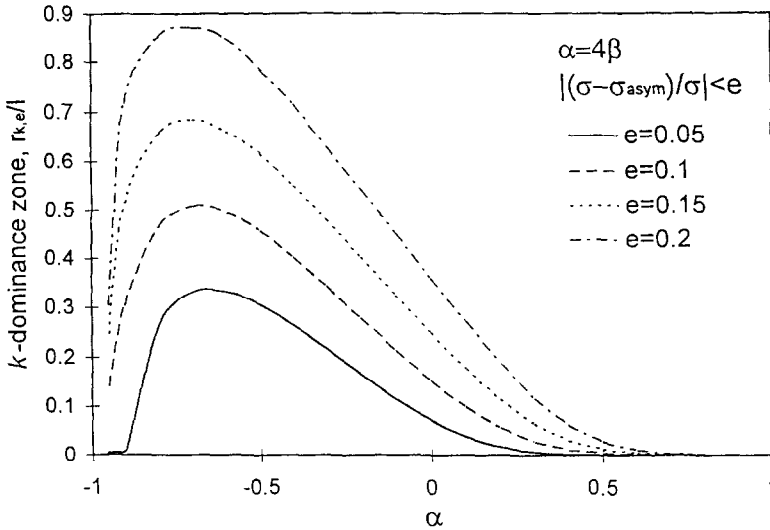


Fig. 7. Zone of  $k$ -dominance for a crack under remote tension.

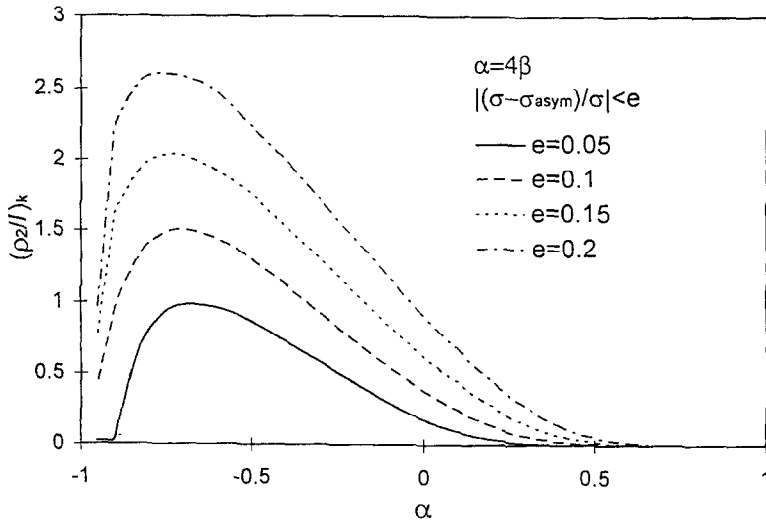


Fig. 8. Admissible  $\rho_2/l$  values for SSY analysis

does not apply for  $\alpha > 0.5$ , due to the lack of a sufficiently large  $k$ -dominated region. An accurate evaluation of the region where the crack tip stresses predicted by the cohesive crack model are approximated by (33) is given in the next section.

For admissible  $\rho_2/l$  values, eqns (26), (29) and (30) can be used to derive the critical far-field stress intensity factor, the non-dimensional critical far-field tension,  $\sigma_{1c}/\sigma_o$ , and the  $\sigma_{1c}/\sigma_c^{hom}$  ratio respectively. The loci of constant  $\Theta(\alpha, \beta)$ , which appears in (30), are shown in Fig. 9. Plots of  $\sigma_{1c}/\sigma_c$  and  $\sigma_{1c}/\sigma_c^{hom}$  as functions of the  $\rho_2/l$  are shown in the boxed inserts of Figs 10 and 11 for various values of  $\alpha = 4\beta$ . An interesting result is that under SSY conditions, the critical far-field stress,  $\sigma_{1c}$ , is a weak function for a broad range of  $\alpha$  values. This suggests that the parameters  $\sigma_o$  and  $\rho_2$  have more control on crack initiation than the strength of the elastic stress singularity at the interface,  $\lambda$ . For instance, at  $\rho_2/l = 0.05$  the  $\sigma_{1c}/\sigma_c^{hom}$  values for  $\alpha = 4\beta = -0.7-0.7$  ( $E'_2/E'_1 = 0.18-5.7$ ) are in the range  $1 \pm 0.2$ . For larger values of  $\rho_2/l$  the characteristic  $\alpha$ -curves tend to spread; however at  $\rho_2/l = 0.2$ ,  $\sigma_{1c}/\sigma_c^{hom}$  values still fall in the range  $1 \pm 0.25$  for  $\alpha = 4\beta = -0.4-0.4$  ( $E'_2/E'_1 = 0.43-2.3$ ).

As expected, for the limiting case of no plastic deformation the linear elastic solution is recovered. As shown in the insert of Fig. 11, for  $\rho_2/l \rightarrow 0$  the  $\sigma_{1c}/\sigma_c^{hom}$  ratio tends to 0 for  $\mu_2 < \mu_1$  ( $\alpha < 0$ ) and  $\infty$  for  $\mu_2 > \mu_1$  ( $\alpha > 0$ ), as predicted by LEFM.

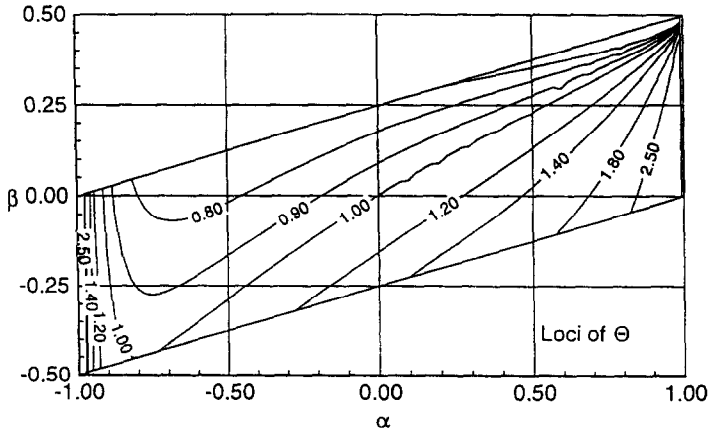


Fig. 9. Loci of constant  $\Theta$  in the  $\alpha$ - $\beta$  plane.

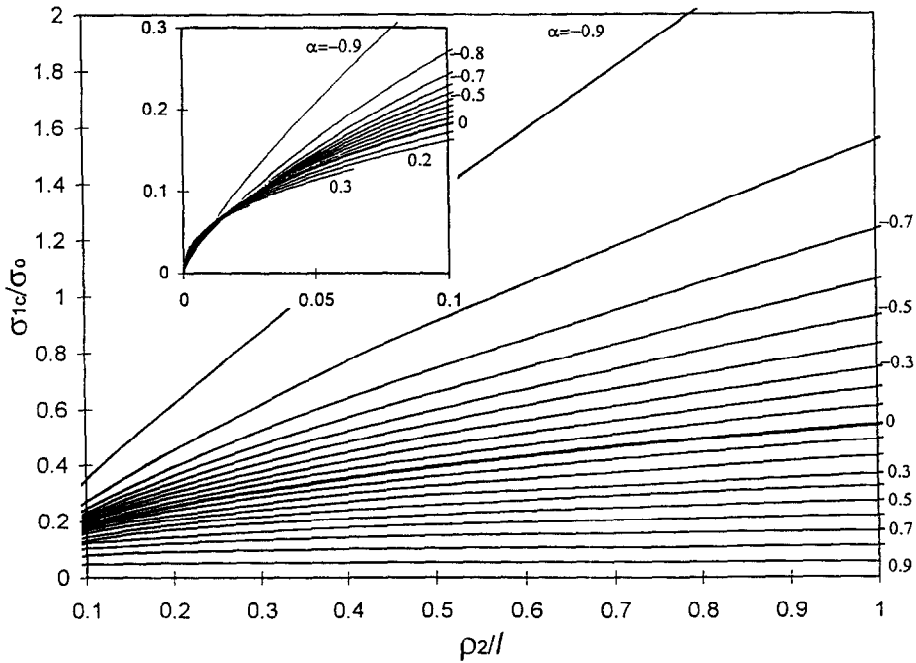


Fig. 10. Non-dimensional critical remote stress,  $\sigma_{1c}/\sigma_0$  as functions of  $\rho_2/l$ .

4. EXTENSION OF THE DUGDALE MODEL TO BIMATERIAL SYSTEMS UNDER LSY CONDITIONS

4.1. LSY model

The validity of the GD model introduced in the previous section is limited to SSY conditions; a different approach must therefore be developed for the case of large crack tip deformation. However, (8) and (9) cannot be directly generalized to the problem of Fig. 5b since universal solutions for the stress intensity factor and crack opening displacement at the interface are not available. For this reason, it is necessary to rely on the direct solution of the integral equations governing the finite length cohesive crack problem, which can be formulated in terms of the unknown dislocation densities

$$b^{(i)}(\xi) \equiv \frac{\partial}{\partial \xi} [u_x^{(i)}] \quad (i = 1, 2) \tag{36}$$

where  $[u_x^{(i)}(\xi)]$  is the crack opening displacement.

The problem shown in Fig. 5b, with  $\sigma^{(1)}$  and  $\sigma^{(2)}$  related by eqn (32), can be analyzed by means of the superposition scheme shown in Fig. 5c and 5d. The loading condition in

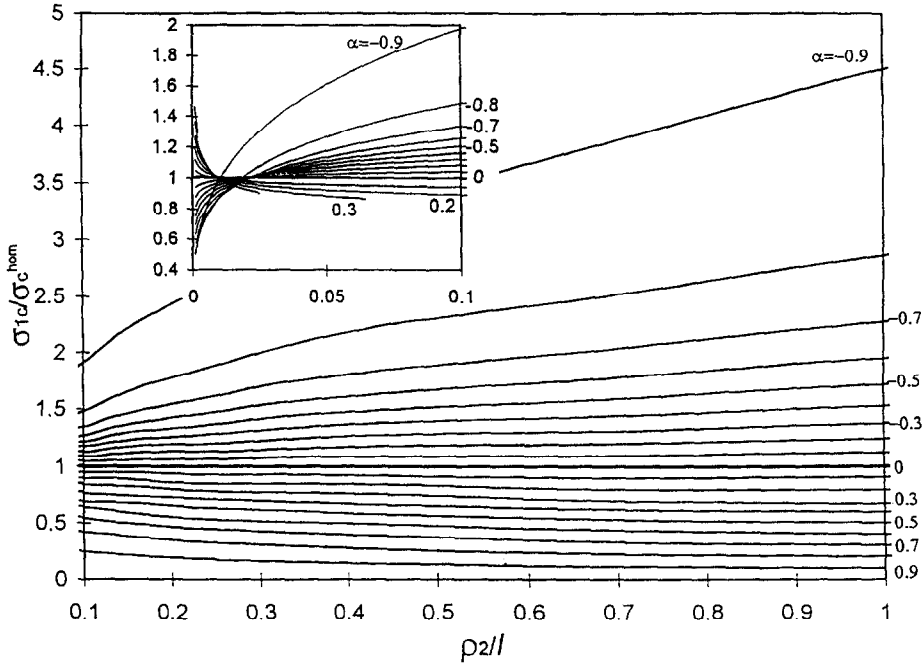


Fig. 11. Normalized critical remove stress,  $\sigma_{1c}/\sigma_c^{hom}$  as functions of  $\rho_2/l$ .

Fig. 5c corresponds to a uniform state of stress in the two half-planes, whereas for the case of Fig. 5d the system of singular integral equations can be written symbolically as

$$E_1 \int_0^{2l} b^{(1)}(\xi) K_{1i} d\xi + E_2 \int_{-\sigma}^0 b^{(2)}(\xi) K_{2i} d\xi = -4\pi\sigma^{(i)} \quad (i = 1, 2)$$

$$\int_0^{2l} b^{(1)}(\xi) d\xi + \int_{-\sigma}^0 b^{(2)}(\xi) d\xi = 0 \quad (37)$$

where  $K_{ij}$  ( $i, j = 1, 2$ ) are Cauchy type kernels,  $\sigma^{(1)} = \sigma_1$  and  $\sigma^{(2)} = \sigma_2 - \sigma_o$ . The first two eqns (37) represent the traction boundary conditions along the crack surfaces, while the third enforces single valued displacements. An additional condition for the dislocation densities at the interface is necessary to insure the correct asymptotic behaviour ; the details are given in the Appendix. Note that in (37) the quantity  $\delta$  is unknown, while the value of the regular part of  $b^{(2)}(-\delta)$ , which is proportional to the stress intensity factor at the tip of the virtual crack extension, is zero, according to the Dugdale-Barenblatt model.

The solution of the singular integral eqns (37) can be readily obtained with a standard Gauss-Jacobi quadrature scheme. This numerical method is appropriate for the case here considered of relatively large plastic deformation ahead of the interface, for which no numerical instability is encountered. On the other hand, due to the nature of the generalized kernels,  $K_{ij}$ , the numerical integration method becomes inaccurate for small  $\delta/l$ , and is therefore unsuitable for SSY conditions. Therefore the SSY model and the direct integration method are complementary. The threshold value of  $\delta/l$  resulting in numerical instability mainly depends on the number of integration points used in the quadrature scheme, even though other factors, such as the level of bimaterial mismatch, may be significant ; the 400-point integration employed in this study was found to break down for  $\delta/l < 10^{-3}$ . Note that for the semi-infinite crack model given in the previous section the numerical solution scheme used to compute the non-dimensional quantities  $f_k, \tilde{\eta}_k, f_{\sigma_o}$  and  $\tilde{\eta}_{\sigma_o}$  is always well behaved.

4.2. SSY-LSY transition and accuracy of the singular elastic solution

The transition from SSY to LSY conditions resulting from gradually increasing the magnitude of the applied load is shown in terms of the stress ahead of the crack in Figs 13–

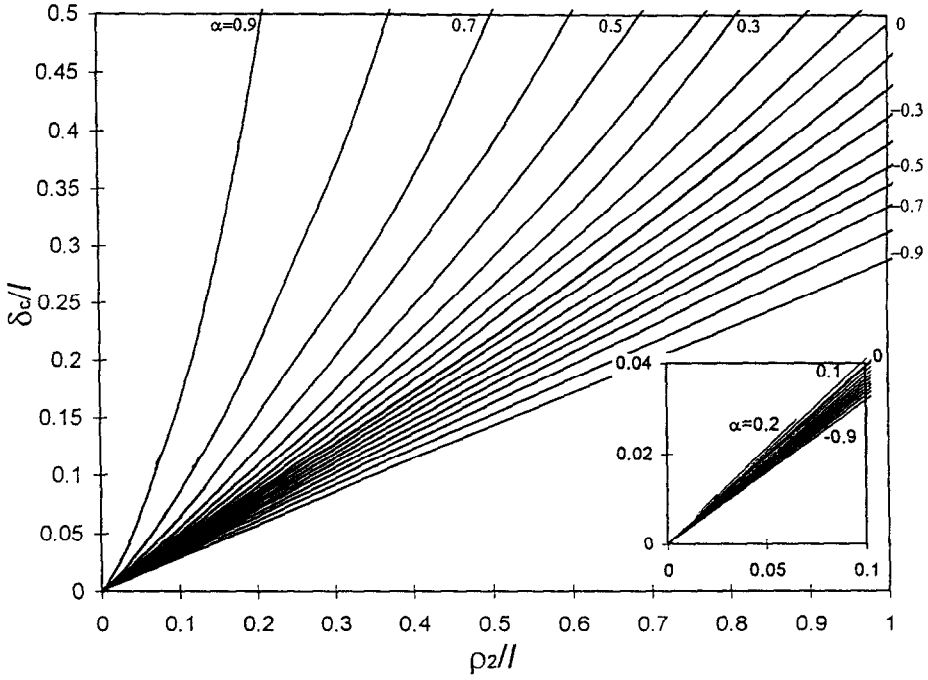


Fig. 12. Non-dimensional length of the cohesive zone,  $\delta_c/l$ , as functions of  $\rho_2/l$ .

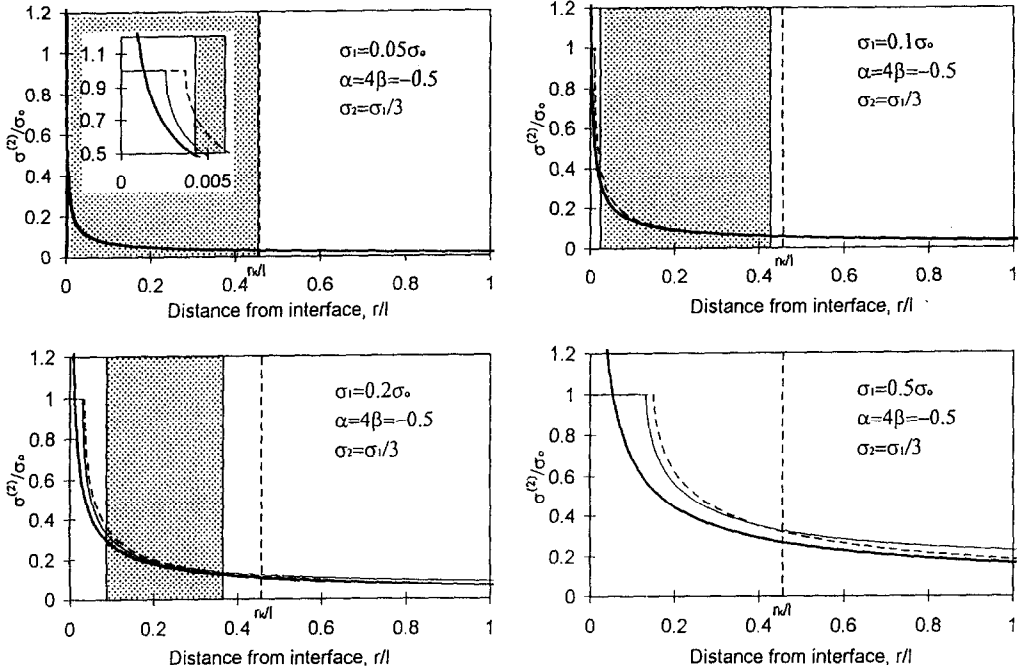


Fig. 13. Crack tip stress fields for  $\alpha = 4\beta = -0.5$ .

15 for three different bimaterial systems,  $\alpha = 4\beta = -1/2, 0$  and  $1/2$ . The stress according to (33), that is the singular term of the elastic solution, is represented in bold, whereas the stress profiles corresponding to the SSY and LSY solutions are represented by the dashed line and the solid line respectively. The boundaries of the  $k$ -dominated region for the elastic problem associated with  $e = 10\%$  are marked by the vertical dashed lines. The shaded areas highlight the region in which the  $k$ -solution and the cohesive crack solution match within

a 10% error; note that for this comparison the appropriate cohesive zone model (SSY or LSY) was chosen for each figure.

(1)  $\alpha = 4\beta = -1/2$

As a first example, consider a bimaterial system with Dundurs parameters  $\alpha = 4\beta = -1/2$  for which  $r_{k,10\%}/l \sim 0.46$ . Figure 13 shows the stress profiles in front of the crack tip for  $\sigma_1/\sigma_o = 0.05, 0.1, 0.2$  and  $0.5$ . It is observed that, compared to the full non-linear solution, the  $k$ -solution provides acceptable stress values in a region that gradually contracts as the critical applied load increases. In fact, for the lowest stress level,  $\sigma_1/\sigma_o = 0.05$ , the singular term of the asymptotic solution is sufficiently accurate in a large region in front of the crack tip, between the values  $r/l \sim 0.0043$  (just ahead of the plastic zone,  $\delta/l = 0.0037$ ) and  $r/l \sim 0.45$ . This region slightly contracts as the loading undergoes a twofold and a fourfold increase ( $r/l = 0.024$  to  $0.43$  for  $\sigma_1/\sigma_o = 0.1$ ,  $r/l = 0.088$  to  $0.37$  for  $\sigma_1/\sigma_o = 0.2$ ) and eventually, for very high applied stresses, it vanishes, as for the case of Fig. 13d relative to  $\sigma_1/\sigma_o = 0.5$ .

Bimaterial systems characterized by the same elastic mismatch but for different  $\rho_2$  reach the state of incipient crack propagation under different magnitudes of the remote stress, depending on the specific value of  $\rho_2/l$ . The four remote stress levels in Figs 13a–d represent the critical crack tip stress fields for bimaterial systems with  $\rho_2/l = 0.01, 0.024, 0.083$  and  $0.37$ , respectively. Note that for the case of Fig. 13b, the SSY and LSY models predictions are very close. For  $\rho_2/l = 0.083$ , Fig. 13c, the SSY solution starts losing accuracy even though it still provides reasonable stress values, while for  $\rho_2/l = 0.37$  it must be replaced by the LSY solution. On the other hand, for  $\rho_2/l = 0.01$  the LSY solution does not provide correct  $\delta$  values; in this case the SSY solution is appropriate.

(2)  $\alpha = 4\beta = 1/2$

The region of  $k$ -dominance, as well as the region of acceptability of the stress predicted by (33), is dramatically reduced for the conjugated bimaterial stress, obtained by switching the two bonded materials ( $\alpha = 4\beta = 0.5$ ). The crack tip stress field for this  $\alpha$ - $\beta$  combination is shown in Fig. 14 for the four loading levels  $\sigma_1/\sigma_o = 0.016, 0.02, 0.03, 0.05$ . From any practical standpoint, it is concluded that for this system, as for most bimaterial combinations with ( $\alpha = 4\beta > 0.4$ ) there is virtually no  $k$ -dominance and that (33) does not provide useful information even for very low remote loading levels.

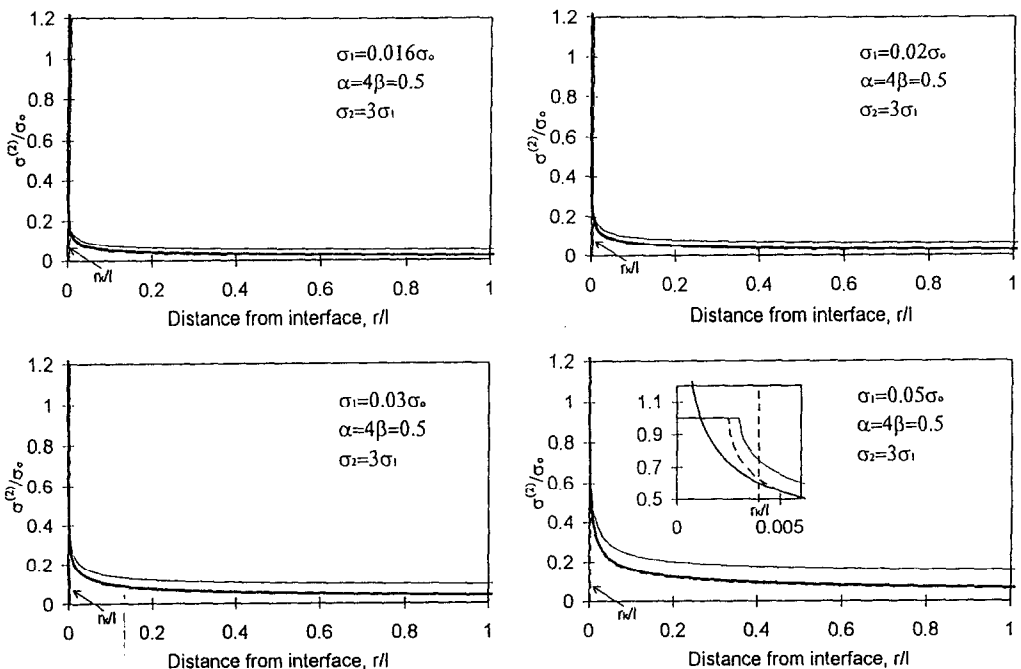


Fig. 14. Crack tip stress fields for  $\alpha = 4\beta = 0.5$ .

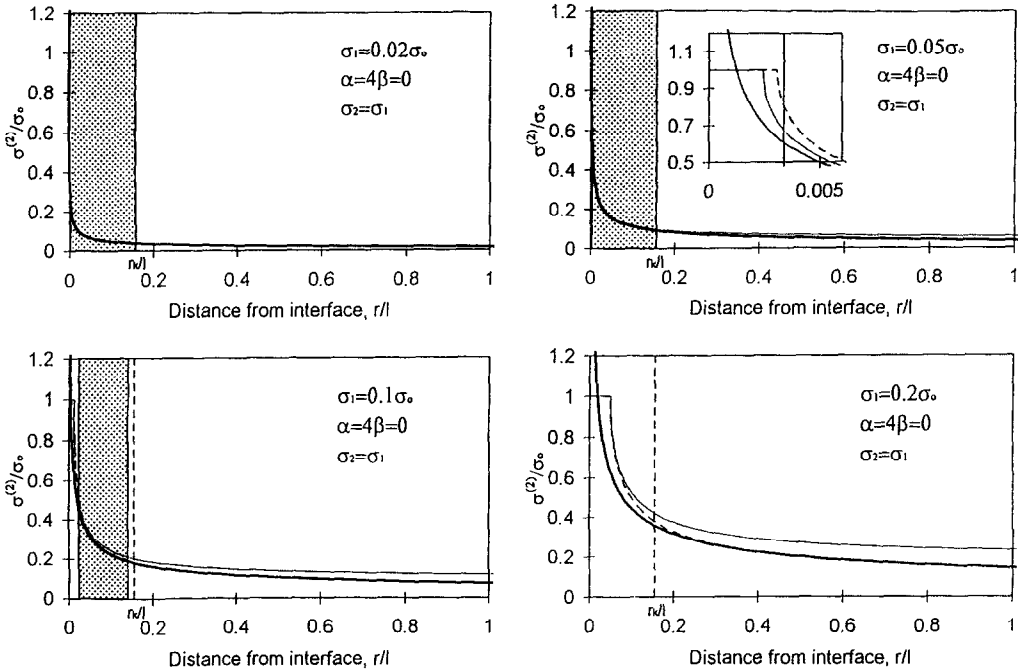


Fig. 15. Crack tip stress fields for  $\alpha = 4\beta = 0$ .

(3)  $\alpha = 4\beta = 0$

Figure 15 shows the results for a homogeneous medium, for which  $r_{k,10\%}/l \sim 0.15$ . Note that for  $\sigma_1 < 0.05\sigma_o$  eqn (33) provides accurate stress values in a region that extends from  $r/l = 0.0031$  (just ahead of the virtual crack tip) to  $r/l = 0.15$ . For higher loads, this region rapidly contracts and disappears, as shown in Fig. 15d for  $\sigma_1 \sim 0.2\sigma_o$ . The four stress levels,  $\sigma_1/\sigma_o = 0.02, 0.05, 0.1, 0.2$ , correspond to the critical load peak for incipient crack propagation of systems with  $\rho_2/l = 0.0013, 0.008, 0.031$  and  $0.126$  respectively. Figure 15a and 15d again show the transition between SSY conditions and LSY conditions.

4.3. Critical stress and cohesive zone length

The critical value of the remote stress  $\sigma_1, \sigma_{1c}$ , normalized with respect to  $\sigma_o$  and the critical stress for the homogeneous system,  $\sigma_c^{hom}$ , for the problem of Fig. 5b is shown in Figs 10 and 11 as functions of  $\rho_2/l$  for various values of  $\alpha = 4\beta$ . The non-dimensional critical length of the cohesive zone,  $\delta_c/l$ , is shown in Fig. 12. It is observed that the SSY solutions, shown in the inserts, exhibit a smooth transition to the LSY solutions obtained by integrating (37).

For LSY conditions, both  $\sigma_{1c}/\sigma_o$  and  $\sigma_{1c}/\sigma_c^{hom}$  are weak functions of  $\rho_2/l$  for a wide range of  $\alpha = 4\beta$  values. Moreover, as already observed for the case of SSY,  $\sigma_{1c}/\sigma_c^{hom}$  is insensitive to the level of bimaterial mismatch even for LSY. For most metallic composites, characterized by  $\alpha < 0.6$ , the critical remote stress,  $\sigma_{1c}$ , is in fact bounded within  $\pm 50\%$  of the corresponding reference critical stress,  $\sigma_{1c}^{hom}$ . For a higher level of mismatch (for instance aluminium composites and plastics composites, which are characterized by  $\alpha > 0.6$ )  $\sigma_{1c}/\sigma_c^{hom}$  may reach considerably high values or values close to zero, depending on the relative stiffness of the bonded materials.

5. CONCLUSIONS

A propagation criterion for cracks terminating at a bimaterial interface has been derived by modeling the fracture process zone ahead of the interface with a cohesive closing pressure. Both the cases of LSY and SSY conditions have been considered. In particular, the SSY propagation criterion is based on the introduction of the bimaterial fracture toughness,  $k_c$ , which has been expressed in terms of the parameters that control the elastic mismatch and inelastic deformation. For a crack of length  $2l$  terminating at a bimaterial

interface, it's been shown that under SSY conditions, the ratio of the critical remote stress to the critical stress for the homogeneous system,  $\sigma_{1c}/\sigma_c^{hom}$ , is sensitive to variations of the inelastic parameter  $\rho_2/l$ , where  $\rho_2$  is proportional to the SSY critical cohesive crack length; for large crack tip deformation this dependence tends to disappear. For relatively small  $\rho_2/l$ ,  $\sigma_{1c}/\sigma_c^{hom}$  is insensitive to the level of material mismatch. For most bimaterial systems with  $\alpha = 4\beta$ , the stress ratio  $\sigma_{1c}/\sigma_c^{hom}$  has been predicted to be in the  $1 \pm 0.5$  range. During the solution of the integral equations it was discovered that the stress intensity factor has a relatively small region of dominance for the case where the crack is in the more compliant material.

## REFERENCES

- Atkinson, C. (1975) On the stress intensity factors associated with cracks interacting with an interface between two elastic media. *International Journal of Engineering Science* **13**, 489–504.
- Barenblatt, G. I. (1962) The mathematical theory of equilibrium cracks in brittle fracture. *Advances in Applied Mechanics* Vol. VII, pp. 55–129, Academic Press.
- Cook, T. S. and Erdogan, F. (1972) Stresses in bonded materials with a crack perpendicular to the interface. *International Journal of Engineering Science* **10**, 677–697.
- Dugdale, D. S. (1962) Yielding of steel sheets containing slits. *Journal of the Mechanics and Physics of Solids* **8**, 100–104.
- Dundurs, J. (1969) Elastic interaction of dislocations with inhomogeneities. In *Mathematical Theory of Dislocations* (ed. T. Mura), pp. 70–114, ASME.
- He, M. Y. and Hutchinson, J. W. (1989) Crack deflection at an interface between two dissimilar elastic materials. *International Journal of Solids and Structures* **25**, 1053–1067.
- Rice, J. R. (1968) A path-independent integral and the approximate analysis of strain concentration by notches and cracks. *Journal of Applied Mechanics* **35**, 379–386.
- Romeo, A. and Ballarini, R. (1994) The influence of elastic mismatch on the size of the plastic zone of a crack terminating at a brittle-ductile interface. *International Journal of Fracture* **65**, 183–196.
- Romeo, A. and Ballarini, R. (1995) A crack very close to a bimaterial interface. *Journal of Applied Mechanics* **62**, 617–619.
- Suga, T., Ellsner, G. and Schmauder, S. (1988) Composite parameters and mechanical compatibility of material joints. *Journal of Composite Materials* **22**, 917–934.
- Wang, Y. C., Hui, C. Y., Lagoudas, D. and Papadopoulos, J. (1991) Small-scale blunting at a bimaterial interface with Coulomb friction. *International Journal of Fracture* **52**, 293–306.
- Zak, A. R. and Williams, M. L. (1963) Crack point stress singularities at a bi-material interface. *Journal of Applied Mechanics* **30**, 142–143.

## APPENDIX

Let:

$$A_i = \frac{2\mu_i}{\pi(1+\kappa_i)} = \frac{E_i'}{4\pi} \quad (i = 1, 2) \quad (\text{A1})$$

$$M = \frac{\alpha + \beta^2}{1 - \beta^2} \quad N = \frac{2(\alpha - \beta)}{1 + \beta} \quad S = \frac{1 + \alpha}{1 - \beta^2} \quad (\text{A2})$$

$$P = \frac{\alpha - \beta^2}{1 - \beta^2} \quad Q = \frac{2(\alpha - \beta)}{1 - \beta} \quad T = \frac{1 - \alpha}{1 - \beta^2}$$

$$K_{11}(\xi, y) = \frac{1}{y - \xi} + \frac{M}{y + \xi} + \frac{\xi(y - \xi)N}{(y + \xi)^3}$$

$$K_{12}(\xi, y) = S \left[ \frac{1}{y - \xi} - 2\beta \frac{\xi}{(y - \xi)^2} \right]$$

$$K_{21}(\xi, y) = T \left[ \frac{1}{y - \xi} - 2\beta \frac{\xi}{(y - \xi)^2} \right]$$

$$K_{22}(\xi, y) = \frac{1}{y - \xi} - \frac{P}{y + \xi} + \frac{\xi(y - \xi)Q}{(y + \xi)^3} \quad (\text{A3})$$

## A1. Semi-infinite crack extending through a bimaterial interface

The problem of a semi-infinite crack extending through a bimaterial interface is governed by the equations

$$A_1 \int_0^\infty b^{(1)}(\xi) K_{1i} d\xi + A_2 \int_{-\delta}^0 b^{(2)}(\xi) K_{2i} d\xi = \sigma^{(i)} \quad (i = 1, 2) \quad (\text{A4})$$

$$\lim_{\xi \rightarrow 0^+} b^{(1)}(\xi)/b^{(2)}(-\xi) = F(\alpha, \beta, \mu) \quad (\text{A5})$$

where

$$F(\alpha, \beta, \mu) = \frac{(1 + \alpha)\beta + (\alpha - \beta)(1 - \beta)(-1 + 4\mu - 2\mu^2) - (1 - \beta^2) \cos(\mu\pi)}{(1 + \alpha)(-1 + 2\beta - 2\beta\mu)} \tag{A6}$$

and  $\mu$  is the power of the stress singularity at the interface, which satisfies the characteristic equation

$$(1 - \beta^2)(1 + \cos^2 \mu\pi) + 2[2\alpha\beta - 1 - (2\alpha\beta - \beta^2) \cos \mu\pi] + 4\mu(2 - \mu)[(\alpha - \beta)^2(1 - \mu)^2 - \alpha\beta + \beta(\alpha - \beta) \cos \mu\pi] = 0. \tag{A7}$$

The loci of  $\mu$  in the  $\alpha - \beta$  plane are presented in Fig. 2b. The unknown dislocation density functions have the form

$$b^{(1)}(\xi) = \frac{k}{\sqrt{2\pi}} \frac{1}{(\xi + \delta)^{\lambda - \mu} \xi^\mu} \left[ \frac{4}{E_1} \tilde{b}^{(1)}(\xi) + w_1(\xi) \psi^{-1} \right],$$

$$b^{(2)}(\xi) = \frac{k}{\sqrt{2\pi}} \frac{4}{E_2} \frac{\tilde{b}^{(2)}(\xi)}{(-\xi)^\mu (\delta + \xi)^{1/2}} \delta^{1/2 - \mu - \lambda} \tag{A8}$$

where  $\tilde{b}^{(1)}$  and  $\tilde{b}^{(2)}$  are regular functions,  $w_1$  is defined in A1.1 and A1.2 as a transition function which depends on the applied loading, and

$$\lim_{\xi \rightarrow \infty} \tilde{b}^{(1)}(\xi) = 0. \tag{A9}$$

$$\psi \equiv \frac{E_1}{4} \frac{1}{\sin(\lambda\pi)} \frac{1 + \alpha}{1 - \beta^2} [1 - 2\beta(\lambda - 1)]. \tag{A10}$$

*A1.1. Semi-infinite crack subjected to remote loading, k.*

For this case  $\sigma^{(1)} = 0$  and  $w_1(\xi)$  is taken as

$$w_1(\xi) = \sin^2 \left[ \frac{\pi}{2} \frac{\xi + \delta}{\xi} \right]. \tag{A11}$$

By extracting the dominant term of the crack tip singularity, the non-dimensional ratio of the local stress intensity factor,  $K_k$ , and far-field stress intensity factor,  $k$ , is given by

$$f_k(\alpha, \beta) = \frac{K_k}{k} \delta^{\lambda - 1/2} = \tilde{b}^{(2)}(-\delta). \tag{A12}$$

The crack opening displacement beyond the bimaterial interface is given by

$$[u_k^{(2)}(\xi)] = \int_{-\delta}^{\xi} b^{(2)}(\zeta) d\zeta = \frac{4}{E_1} k \delta^{1 - \lambda} H(\xi/\delta; \alpha, \beta) \tag{A13}$$

where  $H$  is a non-dimensional function. This last equation provides the value of the crack opening displacement at the interface

$$\eta_k \equiv [u_k^{(2)}(0)] = \int_{-\delta}^0 b^{(2)}(\zeta) d\zeta = \frac{4}{E_1} k \delta^{1 - \lambda} \tilde{\eta}_k(\alpha, \beta) \tag{A14}$$

where  $\tilde{\eta}_k(\alpha, \beta) \equiv H(0; \alpha, \beta)$ .

*A1.2. Semi-infinite crack subjected to uniform cohesive pressure*

For this case  $\sigma^{(1)} = 0$ ,  $\sigma^{(2)} = \sigma_o$ , and  $w_1(\xi) \equiv 0$ .  $k$  disappears as a parameter, and is incorporated in the dislocation density functions. Again, the local stress intensity factor can be derived by extracting the dominant term of the crack tip singularity as

$$K_{\sigma_o} = \sigma_o \sqrt{2\pi\delta} \tilde{b}^{(2)}(-\delta) = \sigma_o \sqrt{2\pi\delta} f_{\sigma_o}(\alpha, \beta). \tag{A15}$$

The crack opening displacement at the interface is given by

$$\eta_{\sigma_o} = \int_{-\delta}^0 b^{(2)}(\zeta) d\zeta = \frac{4}{E_1} \sigma_o \delta \tilde{\eta}_{\sigma_o}(\alpha, \beta). \tag{A16}$$

*A2. Finite crack subjected to uniform cohesive pressure*

The integral equation formulation for the problem of Fig. 5d is given by (A4) with the upper limit  $\infty$  replaced by  $2l$ . At the right hand side,  $\sigma^{(1)} = \sigma_1$  and  $\sigma^{(2)} = \sigma_o - \sigma_1/C$ . For this case the dislocation densities have the form

$$b^{(1)}(\xi) = l^{1/2+\mu} \frac{\tilde{b}^{(1)}(\xi)}{\xi^\mu (2l-\xi)^{1/2}}$$

$$b^{(2)}(\xi) = (\delta/2)^{1/2+\mu} \frac{\tilde{b}^{(2)}(\xi)}{(-\xi)^\mu (\delta+\xi)^{1/2}} \quad (\text{A17})$$

where  $\tilde{b}^{(1)}$  and  $\tilde{b}^{(2)}$  are regular functions. Equation (A5) is unchanged, while the far-field condition (A10) is replaced by

$$\int_0^{2l} b^{(1)}(\xi) d\xi + \int_{-\delta}^0 b^{(2)}(\xi) d\xi = 0 \quad (\text{A18})$$

which enforces single valued displacements.